

Medical Image Segmentation Algorithm Based on Markup Improvement Combining the Watershed Algorithm and the Level Set Algorithm

Yanyan Wu^{1,a,*}, Qian Li^{2,b}

¹College of Digital Technology and Engineering, Ningbo University of Finance and Economics, Ningbo, China

²College of Digital Technology and Engineering, Ningbo University of Finance and Economics, Ningbo, China

^awuyanyan@nbufe.edu.cn, ^bliqian@nbufe.edu.cn

*Corresponding author

Abstract: In this paper, a method is proposed to merge the level set segmentation and the watershed segmentation for edge detection in medical images. To solve the issue of over-segmentation in the watershed algorithm, this improved watershed algorithm is proposed. By identifying the foreground and background, the number of segmented zones can be adjusted. For the process of filling the valley bottom, the divided region's contour is enhanced and modified to ensure that it fits as closely as possible to the target edge. The location of the edge in the gradient map is enhanced and adjusted, while the largest connected region is applied to acquire image edge information. Experiments have shown that this technique can reduce over-segmentation in medical images.

Keywords: Medical Image Segmentation, Mark, Watershed Algorithm, Level Set

1. Introduction

A relatively active subfield of image segmentation is medical image segmentation. By removing the features of the segmentation target, the aim is to distinguish the region of interest from the surrounding area. The accuracy of clinical diagnosis and therapy is directly related to the results of medical image segmentation. The ability of segmentation to meet clinical needs and provide real-time interactive tools for physicians is correlated with segmentation speed. The accuracy and reliability of segmentation is directly associated with the robustness of the algorithm. In a clinically challenging environment, the evaluation criteria of image segmentation algorithms are closely related to accuracy and reliability. The efficiency of the algorithm is closely associated with the level of automation. In addition to ensuring reliable accuracy, it is used in a clinical environment.

In this study, we propose an edge detection method for medical images combining level set and watershed segmentation. The following two main points explain how the proposed method differs from existing segmentation methods proposed in the literature. (1) It is intended to be an adaptive and economic solution with effective algorithmic components. (2) It is suitable for both common and medical images. In addition, the proposed method outperforms other effective methods in medical image segmentation due to the implementation of our improved algorithm.

An image segmentation method combining the watershed algorithm and the level set algorithm is proposed by extracting the most connected region of the segmentation. The result of the watershed algorithm becomes the initial evolution curve of the level set algorithm, which combines the enhanced watershed algorithm with the improved model. In addition to increasing the effectiveness of segmentation, this technique also increases the precision.

The manuscript is structured as follows. The basic explanation of image segmentation, watershed segmentation, level set and a brief introduction to the basic techniques used in medical image segmentation are given in the second section. Our new approach is described in section 3, which combines the watershed algorithm to extract the maximum connectivity with the level set technique to perform curve evolution. In this study, the pre-processing phase of the marker-based watershed technique is mainly improved. Sections V and VI both cover the experimentation results based on level sets and watershed segmentation. Finally, section VII presents the conclusion.

2. Related work

Image processing and recognition is at the forefront of high technology. Image recognition research addresses the inability of human physiological organs to detect problems by using computers to automatically interpret a large amount of physical information, partially replacing the work of the human mind.

2.1. Image segmentation

Image segmentation refers to segmenting an image region into non-overlapping and interconnected regions with uniform signal characteristics ^[1]. Image segmentation is one of the challenging problems in computer vision, especially in the field of medical image segmentation. The principles of medical imaging are inherently subject to the effects of noise, the field offset effect and the local body effect. Due to the complexity of human tissues and individual differences, tissue mobility and other variables will also affect images. Medical images differ from other images in that they have poor contrast, uneven grey levels, excessive noise, blurred edges, etc. As a result, the field of medical image segmentation faces greater challenges. When segmenting medical images, which are composed of many elements and imaging techniques, it is difficult to get better results. To solve these problems, it is necessary to explore the many medical image segmentation approaches, understand the advantages and disadvantages of each approach, and then improve each approach by thoroughly studying the particular processing strategies used in each process. The segmentation accuracy and speed of different segmentation algorithms are also important research issues. The technique for segmenting medical images is therefore an ongoing problem.

2.2. Watershed algorithm

The image segmentation algorithm known as "watershed segmentation" ^[2] combines geomorphology and regional development. In this method, a grey image is considered as a "topographic map" that combines geomorphology and regional development. In this method, a grey image is considered as a topographic map. Mountains are represented by pixel regions with high grey values, and lowlands are represented by pixel regions with low grey values. Suppose that during the rainy season, water flows from high mountains to low-lying regions, creating 'lakes' called catchment areas. It's possible for water to overflow into neighbouring basins when the water level in one rises. Any intersection of basins can be protected from flooding by building a dam, and segmentation of the image produces a dividing line that marks where these DAMS are located.

2.3. Basic operations of morphology

Expansion, corrosion, opening and closing, and gradient operations are among the fundamental processes of morphology ^[3].

(1)(Expansion) operation: The structural elements are represented by the opening creates $f(x, y)$ greyscale image. Expansion is an arithmetic operation on the edges of the objects in the transformation, specifically the edge of the object where $\max(f + b)$ output values have been selected.

$$(f \oplus g)(x, y) = \max\{f(x - i, y - j) + b(x, y)\} \quad (1)$$

Inflation produces an image that is brighter and larger $(f \oplus g)(x, y)$ than the original image $f(x, y)$. If the structural element of the pixel value is greater than zero. These two results of the expansion operation are possible. The comparatively low gray scale of the pixels in the original image $f(x, y)$ is reduced or eliminated after the expansion operations.

(2)(Corrosion) operation: Expansion and corrosion on the other hand, corrosion is arithmetic of the image $f(x, y)$, the edges of the transformed objects, namely at the edge of the object selected $\min(f - b)$ as output values.

$$(f \ominus g)(x, y) = \min_{i,j}\{f(x - i, y - j) - b(-i, -j)\} \quad (2)$$

The result of the corrosion calculation can be as follows:

Compared to the original image $f(x,y)$, corrosion occurs when the structural components of the

pixel value are greater than zero. It's dark. After the corrosion calculation, pixels in the original image $f(x,y)$ with a particularly high grey value will have their strength reduced or even removed.

(3)(Open/close) operation: Erosion and opening can be used to create the open/close process of greyscale morphology, which is analogous to binary morphology.

$$\text{(Opening)} \quad f \circ g = (f \ominus b) \oplus b \quad (3)$$

$$\text{Closing)} \quad f * g = (f \oplus b) \ominus b \quad (4)$$

(4)(Gradient) operation: After subtracting the corrosion of f and b , which occurs after their expansion, the morphological gradient g can be derived.

$$g = (f \oplus b) - (f \ominus b) \quad (5)$$

2.4. Basic operations of level set technique

The level set technique was first introduced in 1988 by Osher and Sethian to define the curve evolution process^[4]. The use of the level set of three or more dimensions to describe the curve evolution of two dimensions and to provide the implicit representation of the curve evolution is the basic mathematical definition of the level set algorithm. Taking the plane closed curve $C(p, t) [x(p, t), y(p, t)]$ as an example, in the level set algorithm, it is implicitly expresses it as the zero sets of the function value $z=0$ in the three-dimensional function surface $z=(x, y, t)$, i.e., the intersection line between the three-dimensional function surface and the XY plane. Known as the zero level set, $(x, y, t) = 0$, known as the level set function to $C(p, t) = \{(x, y, t) | (x, y, t) = 0\}$.

The mathematical expression for a level set can be expressed as follows: Assuming that the function (x, y, t) is an equation on a three-dimensional space and the line (x, y, t) is equal to 0, $x, y \in \partial\mathcal{E}$, then the level set function (x, y, t) satisfies the following characteristics^[5]:

$$\begin{cases} \phi(x, y, t) < 0, (x, y) \in \mathcal{E} \\ \phi(x, y, t) > 0, (x, y) \in \bar{\mathcal{E}} \\ \phi(x, y, t) = 0, (x, y) \in \partial\mathcal{E} \end{cases} \quad (6)$$

It has many applications, such as fluid dynamics, animation, computer graphics, especially in medical graphics. The advantage is that object boundaries are well represented. For example, its smoothness and closure make it suitable for shape analysis and recognition. It is capable of using sophisticated mathematical techniques, including variational methods, partial differential equations and differential geometry.

2.5. Prewitt operator

The Prewitt operator is often used in the edge detection of image difference operators, which first calculate the average value and then the difference value to determine the gradient. The concept of the Prewitt operator uses the difference between the grey values of pixels in a given area. Its implementation principle is achieved by testing the horizontal direction and the straight direction in two directions, using the neighbourhood convolution between the sample and the graph in the graph region.

3. Method

3.1. New algorithm description

A watershed algorithm, also known as a watershed transformation, is a segmentation technique based on the mathematical theory of morphology and according to the geographical characteristics of the image. It was at this time that a watershed algorithm was introduced into the field of image processing, and since then it has evolved considerably^[6]. Subsequently, the work of Vincent, Soille, and Beucher et al. led to the development of a perfect watershed algorithm theory and an order of magnitude increase in the computational speed of the original watershed algorithm.

Watershed based image segmentation method has a light computational burden. Split the advantages of high accuracy, but typically due to image noise and local irregularity, the number of local minimum will be greater than the actual target, resulting in a lot of false contours, interfering with the actual contour recognition, and also appear over-segmentation phenomenon, making it difficult to split the outline of recognition based on the actual target. It has caused some obstacles to the wide application of the algorithm.

A watershed technique that employs the markers obtained from the gradient's low frequency component to rectify the original gradient image has been put forth in the literature [7]. This method combines the morphological minimum calibration approach with the second-order Butterworth low-pass filter. The watershed approach was then used to process the enhanced gradient image. Despite the better results, problems such as illumination and incorrect edge positioning still exist and cannot be avoided. In reference [8], h-minima technology was integrated with fuzzy distance transformation for watershed segmentation to create markers, but certain pseudo-minima values remained in this technique. In literature [9], a morphological multiscale gradient approach was proposed, which handled step edges and fuzzy edges well, but did not completely remove false edges. According to literature [10], the edge position of the gradient map can be improved and corrected by modifying the fill level and applying the canny operator to capture the edge information of the image, but the contour of the object is still missed.

This research primarily improves the pre-processing watershed algorithm based on the marker. The original image is processed using the corrosion filter and the expansion filter in the morphology before the algorithm is executed. The original image is then combined with the corroded image and the expansion image, and the combined image is then opened and closed to produce the pre-processed image. A marker-based watershed method is then applied to the pre-processed image. The edge of the largest area curve is extracted from the segmentation results produced by the modified watershed technique and used as the initial curve for level set evolution. An improved fast level set algorithm is used for curve evolution. Figure 1 depicts how the method used in this paper flows.

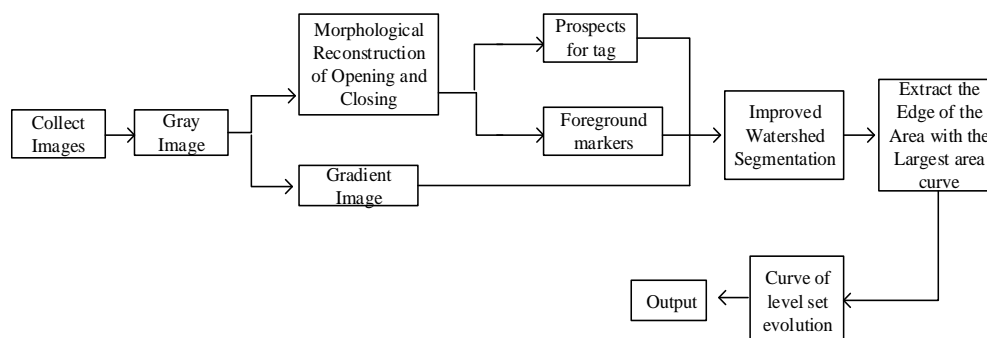


Figure 1: The improved image segmentation procedure of the new algorithm

3.2. LBF model

The LBF model uses the pixel weighting data of the local region and adds the Gaussian kernel function to the energy function. The range of the grey level region that can be fitted by the hybrid level set model is determined by the parameter size of the non-negative kernel function. When the fitting energy of point X reaches its minimum and the evolution curve C reaches the target boundary, the grey value fitted by the curve will be close to the grey values inside and outside the curve. As a result, the target boundary can be determined as long as all points in the region have the lowest fitting energy.

The local binary fit energy in the LBF model, which uses it as the local energy functional, takes the role of the global two in the PC model value-fit energy. Consequently, the following definition applies to the LBF energy functional:

$$\varepsilon_x^{LBF}(\phi, f_1, f_2) = \lambda_1 \int_{in(c)}^c k(x-y) |I(y) - f_1(x)|^2 dy + \lambda_2 \int_{out(c)}^c k(x-y) |I(y) - f_2(x)|^2 dy \quad (7)$$

Among these, the kernel function $K(x) = K(|x|)$ represents the greyscale values of the image at point x. The local property of $\lim_{x \rightarrow 0} K(x) = 0$ and non-negative single subtraction is present in the kernel $K(x)$. $f_1(x)$ and $f_2(x)$ has local properties whose magnitude is mostly influenced by the grey

value near the point x .

Next, we describe the improved LBF model. It is relevant because in the LBF model, the kernel function $K(x)$ essentially determines how fast the level set evolves. The choice of the kernel function of is crucial. The kernel function chosen in is a Gaussian function^[11]:

$$k_{\sigma}(u) = \frac{1}{\sqrt{2\pi}\sigma} e^{-\frac{u^2}{2\sigma^2}}, u \geq 0 \tag{8}$$

Several obvious features of Gaussian function on two-dimensional image are as follows:

(1) It is a monotonically decreasing function. It will eventually go to zero indefinitely.

(2) When $u = \sigma$, the image has an inflection point (from upper convex to lower convex).

(3) With the increase of the $|u|$, $k_{\sigma}(u)$ drops rapidly, it has three times value of σ . When $|u| \geq 3\sigma$, $K(u) \cong 0$.

Feature (1) must be satisfied by the kernel function. At the same time, since it is not necessary for the point with a distance of σ from the centre X to implement the same processing method with X . Feature (2) is not always required. In addition, feature (3) is not required since the processing of the point that is more than three distances from the centre of X cannot be disregarded. Overall, the slow rate of evolution can be attributed to features (2) and (3).

To improve the evolution speed of the LBF model, the following functions are selected as kernel functions:

$$k_p(u) = \frac{1}{1 + u^p}, p \in (0, 1], u \geq 0 \tag{9}$$

For the kernel function $k_p(u)$, the kernel function $k_p(u)$ is similar to the Gaussian function $k_{\sigma}(u)$. When $p \in (0, 1]$, the kernel function $k_p(u)$ meets the requirements of the Gaussian function $k_p(u)$, which monotonically decreases and eventually drops to zero indefinitely. There is no inflection point. It doesn't has the character of 3σ . Therefore, the kernel function $k_p(u)$ of $p \in (0, 1]$ is chosen to replace the Gaussian function here.

3.3. Image preprocessing

In this study, corrosion and expansion filtering are used to pre-process the original image in order to increase the grey level difference of the image, extract the features of the region boundary more effectively, and achieve a better segmentation effect. Here, the original images produced by corrosion and expansion filters are referred to as "corrosion images" and "expansion images", respectively.

The original image is combined with the expansion and corrosion images to enhance the changing part of the image. It increases the contrast of the target in the image. The special procedure involves adding the original and corroded images and deleting the expanded images. The merged image is the result of the combination. In addition to highlighting changes and increasing contrast, the merged image also draws attention to noise. Not only does it exacerbate the segmentation process, but it also quickly leads to over-segmentation of the target. Therefore, it is important to reprocess the combined image to make the region containing the same mark as much as possible a single piece. This work uses morphological open and close operations coupled with filtering to further process the combined image to achieve its goal, and the resulting image is referred to as the pre-processing image.

Gradient calculation requires the use of appropriate gradient operators for image edge detection. Two templates in the x (horizontal) and y (vertical) directions, referred to as xG and yG , respectively, forma gradient operator. The Prewitt, Laplacian, Sobel, and Gauss-Laplacian are some edge operators that are commonly used^[12]. The gradient image can be obtained by using the Prewitt operator to detect the edge of the pre-processed image.

To achieve the best watershed result, the gradient image is modified below from two views of the valley bottom and mountain top, respectively. Image after operation, after the morphological operator

in filtering out noise, while at the same time with the characteristics of the morphological operator can to some extent, part of the image, and will be reflected in the mountain in the part of the gradient image, but the inevitable weaken or even eliminate the edge with the surrounding the edge pixel gradient drops. It is quite possible that the initially weak peak will be completely 'submerged' in the surrounding pixels during the subsequent valley bottom filling phase, leading to the deviation or even disappearance of the associated edge line in the watershed results. With Canny, the operator has a more precise and thorough ability to recognise edges^[13]. Although the image is processed by an array of morphological operators to reduce the noise interference to some extent, it is inevitable that some small valley bottoms with low gradient will be generated in the gradient image due to some small fluctuations in gray level or quantization errors in the original image, leading to the over-segmentation characteristic in watershed results^[14-16]. The method used in this study selectively fills some valley bottoms based on the valley bottoms. It reduces the number of valley bottoms in the gradient graph due to the small gradient difference between these "fake" valley bottoms and the surrounding pixels^[17].

In this paper, Euclidean distance is used to transform gradient images. The formula for the minimum neighbourhood distance between the region pixel (a, b) and the boundary pixel (k, L) in Euclidean distance is shown below.

The external marker is the zero element set of the image obtained by watershed segmentation.

$$d(m, n) = \sqrt{(a - k)^2 + (b - l)^2} \quad (10)$$

The extended h-maxima transform was used to compute the internal markers. The extended H-maxima transform is performed after the pre-processed image data has been subjected to the H-maxima transform. In fact, the H-maxima transform is used to reconstruct the image data I. To reconstruct the image, first the threshold H is removed from the new data collected after the image data I, and then the maximum local value of the restored image is determined^[18-20].

3.4. Improved algorithm implementation process

In this paper, the forced minimum technique is used to modify the gradient image to obtain a reconstructed gradient image. The function `imimposemin` can be used to implement the forced minimum technique. The syntax of the function call is `mp = imimposemin(f, BGM | FGM)`. MP is the reconstructed gradient image. F is the gradient image obtained by morphological gradient computation. BGM is the external marker. FGM is the internal marker. The reconstructed gradient image is then segmented using the control marker watershed approach^[21], and the resulting image represents the segmentation result in its entirety. This section explains the details of the algorithm. It mainly includes the steps of improving the algorithm, the algorithm of the maximum connected number, and the steps of the level set.

The connected region with the largest area gained is given to the initial curve of the level set, and the level set evolution begins. The level set evolution steps are as follows^[22]:

(1) According to the initial curve, the level set is initialized.

(2) The curve evolution is carried out by using the improved LBF model level set method. That is, the level set ϕ^n at time of C^n is updated. Therefore, ϕ^{n+1} is the level set at the next moment and find the zero level set for n+1 and get the evolution curve C^{n+1} .

(3) First, we need to check whether it is satisfied with $C^n = C^{n+1}$. If yes, the evolution of the curve ends. The curve is called the contour of the target. Otherwise, we set $n = n+1$ and return to Step 2 to continue the evolution.

4. Experiment

4.1. Experimental environment and data setting

Experimental environment: The segmentation effect of the modified marked watershed approach was tested using MATLAB 2016a on a PC with a Core i5-8250U CPU and 8 GB of Memory.

Kaggle dataset: The experimental data set was derived from the Kaggle dataset. This study is based

on two-dimensional images from the Kaggle dataset. The dataset collected two-dimensional images of manually segmented lung images. The 2017 Kaggle Data Science competition involved processing and trying to find lesions in lung CT and brain images. The dataset provided over 1,000 low-dose CT images from high-risk patients displayed in DICOM format.

4.2. Watershed algorithm based on improved morphology

The watershed algorithm based on morphology was compared [23-25], and the lung image in the MATLAB toolbox was evaluated by scrutinising the experimental procedure and results to confirm the validity of the experimental results. Specific operation procedure:

- (1) Grey scale image of the lung;
- (2) The gradient image of the lung is obtained using the Sobel operator;
- (3) The grey image of the lung was filtered and smoothed using the 12*12 slice structural elements by morphological open reconstruction and morphological closed reconstruction;
- (4) The local maximum binary image of the filtered image is acquired. The local minimum area with a number of pixels less than 20 in the image is deleted to create the foreground marker graph. To smooth the edges, the local maximum binary image is subjected to an open and close operation.
- (5) In the third stage, the Otsu method was used to determine the threshold of the filtered image, after which the binary image was obtained [26]. The binary image was subjected to distance transformation and watershed segmentation, with the water dividing line image acting as a background marker;
- (6) The mandatory minimum technique was used to modify the gradient image obtained in step 2, using the MASK as the foreground and background markers;
- (7) The result of step 6 is divided into watersheds;

4.3. Comparison of medical image segmentation between our improved algorithm and other algorithm

The sample data from the Kaggle dataset is used to compare the segmentation results of lung image one and lung image two in Figures 2 and 3 using the edge extraction method and the Prewitt operator. The improved watershed algorithm is used in this paper to compare the segmentation results. It is shown in Figures 2 and Figure 3.

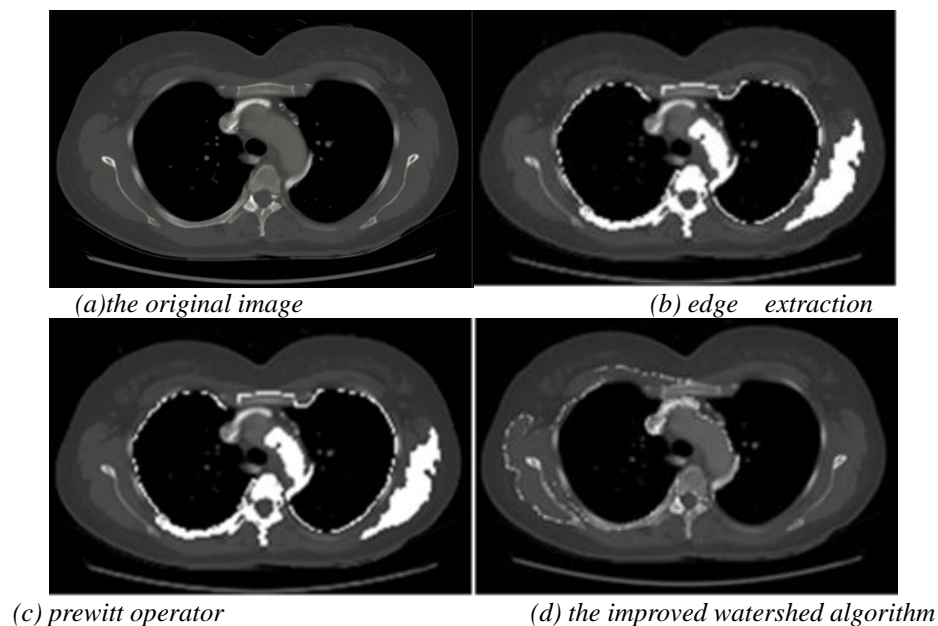


Figure 2: Comparison of segmentation results of lung image one.

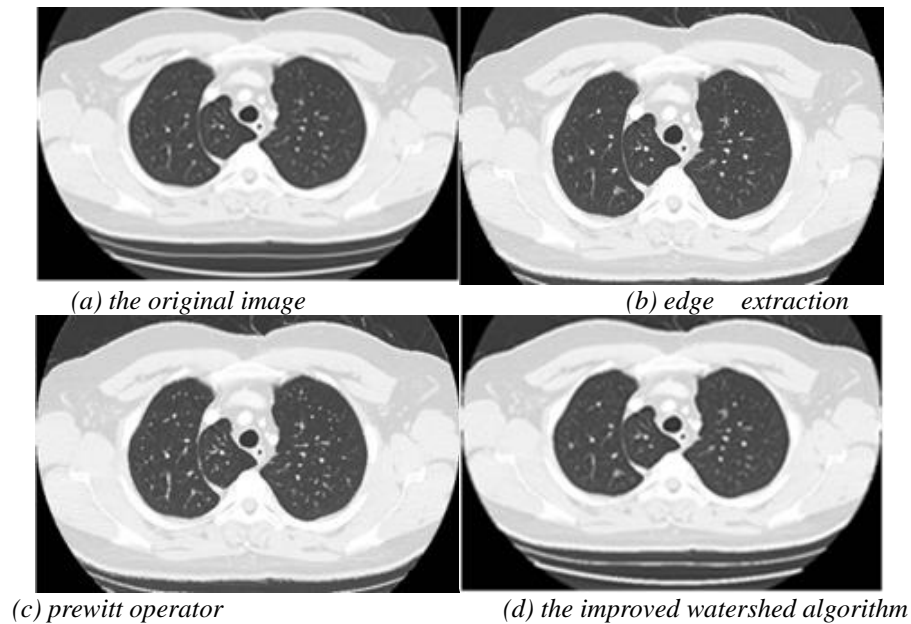


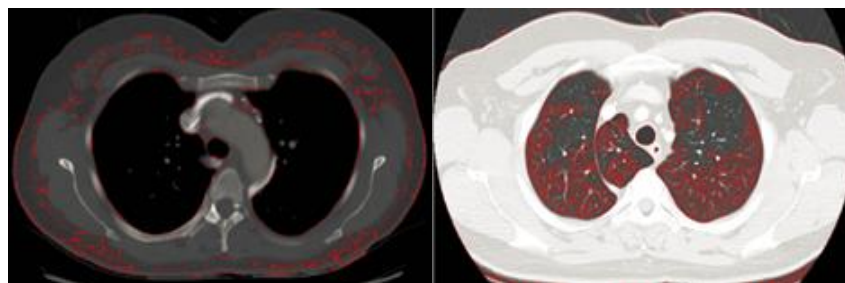
Figure 3: Comparison of segmentation results of lung image two.

In this experiment, the segmentation results of the images in the the Kaggle dataset were compared using the edge extraction approach, the Prewitt operator and the algorithm presented in this research. The comparison results of the original image and the segmented image are shown in Figures 2 and Figure3. Figure2(b), formed by the edge detection algorithm, can effectively extract the edge information of image Figure2(a). Figure2(b) has multiple edge response points, resulting in blur and discontinuity of the edge, which requires further optimization. The edge detection algorithm is sensitive to noise, and it is easy to misidentify noise as edge, resulting in false and missing detection.

The edge extraction algorithm is susceptible to segmentation voids in the process of target segmentation, as shown in Figure3, which can be seen by comparing the experimental results in Figure2(b) and Figure3(b).The segmentation target may also lose some regional information if the segmentation void is too large, as shown in Figure3(b).The results of segmentation using the Prewitt operator and clustering are comparable. However, it is also easy to include too much background information, as shown in Figure2(c) and Figure3(c), making it difficult to understand the essential purpose of the segmentation process. If the grey value difference of the target segmentation is too large, the two types of algorithms mentioned below could lose some information to a certain extent. The improved watershed algorithm forms Figure 2(d) and Figure 3(d), and the image segmentation effect is better than the previous two algorithms, and the robustness is good.

4.4. Getting the maximum connected area

The maximum connected region i extracted from the segmentation results of the improved watershed algorithm. The results are shown in Figure 4.



(a)Maximum connected region of lung one (b) Maximum connected region of image lung image two

Figure 4: Result graph of maximum connected region (the part of red curve)

4.5. Obtain the initial curve and iterate the level set

The largest connected region is used as the original evolution curve of the level set method to evaluate the segmentation performance of the algorithm in images with complicated backgrounds. Several images with complex backgrounds are selected for testing [27-29]. Finally, the fast level set algorithm is used for the image segmentation algorithm model.

The specific processing procedure of this model is as follows:

(1) After removing the original image to be segmented, the modified watershed algorithm is used to segment the original image.

(2) The modified watershed algorithm's segmentation results are processed to create the level set evolution's beginning curve, from which the edge curve of the region with the largest area is retrieved.

(3) Initialize the level set based on the starting curve;

(4) Use the improved fast level set ϕ^n algorithm for curve evolution, which updates the level set at moment N (corresponding to the curve C^n) to the level set ϕ^{n+1} for the next moment to find its zero level set, that is, the evolved curve C^{n+1} ;

(5) Check whether $C^n = C^{n+1}$ is satisfied. If so, the curve's evolution comes to a halt. It serves as the target contour; otherwise, let $n=n+1$ and go back to step 4 to continue the evolution;

LBF models with different initial curves were used to segment medical images of the lungs, and the segmentation results are shown in Figure 5 and Figure 6.

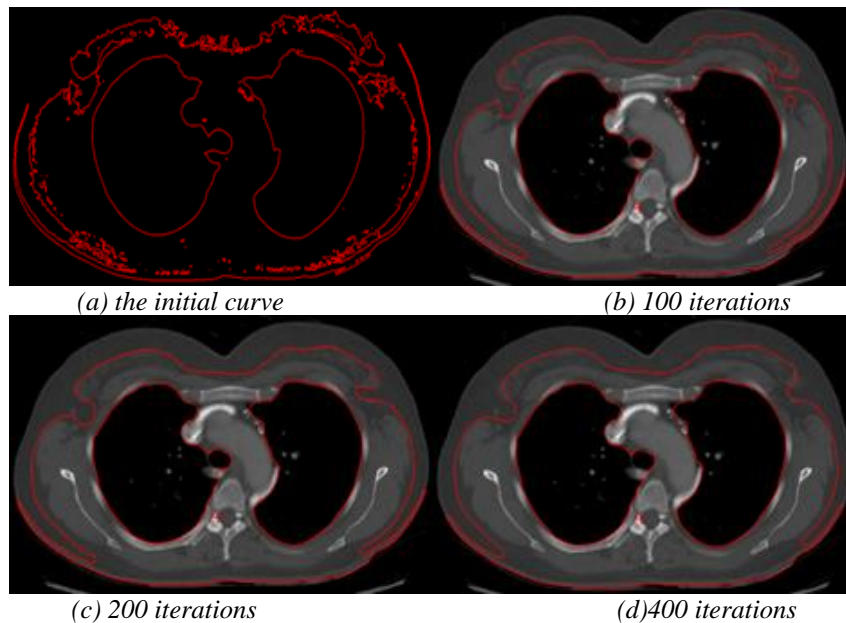
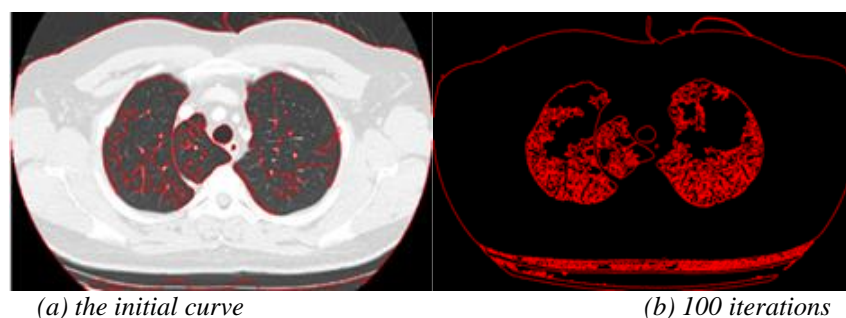


Figure 5: Initial curve LBF segmentation result of lung image one



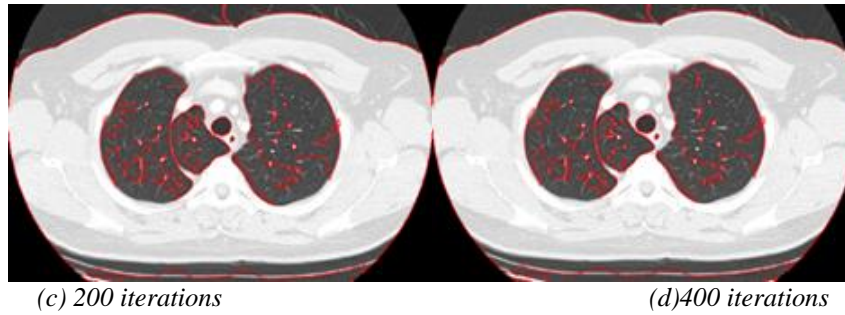


Figure 6: Initial curve LBF segmentation result of lung image two

Comparing the segmentation results of different initial curves in Figure5(a) and Figure6(a), it can be seen that the initial curve from Figure5(a) and the initial curve from Figure6(a) give different results. As can be seen, the choice of initial curve has a significant impact on the segmentation results of the image; different initial curve sizes can produce different segmentation results, with a large initial curve clearly producing better segmentation results than a small initial curve. The segmentation results show that the lesion area of the LBF model segments the data effectively, but is more sensitive to noise. Comparison of the segmentation results shows that the LBF model performs better in segmenting lung lesions in medical images.

5. Result

5.1. Evaluation index

In order to ensure the accuracy of image segmentation, six images can be selected at one time for image segmentation. In order to evaluate the segmentation effect of the algorithm more intuitively, accuracy and recall rate were used to evaluate the three algorithms^[30]. Where accuracy represents the region segmented by the algorithm and the percentage of the target region to be segmented, the formula can be expressed as

$$TP/(TP+FP) \quad (11)$$

TP means true positive. It refers to the exact number of pixels which are identified as the target area. The number of pixels labeled "FP" (false positive) that were mistakenly identified as the target area.

The recall rate, which is the proportion of the target region that the algorithm successfully segments, is defined as

$$TP/(TP + FN) \quad (12)$$

Where FN (False Negative) is the number of pixels that are incorrectly identified as non-target regions.

IoU is a typical performance measure for object class segmentation problems. IoU, which is defined by the following equation, determines the degree of similarity between expected and actual regions of objects contained in a set of images.

$$IoU = TP / (TP + FN + FP) \quad (13)$$

The average segmentation time, segmentation crossover ratio, accuracy, and recall rate of the algorithm were used to make a quantitative comparison of several algorithms.

5.2. Comparison of Average Execution Time of the Algorithm

Table 1: Comparison of algorithm average execution time/s

Image	Edge Detection	Prewitt Operator	Our improved algorithm
Lung image one	2.73	2.86	2.56
Lung image two	3.88	3.54	3.2

We can see from the experimental data in Table 1. The proposed algorithm has certain advantages in the segmentation effect of image details compared to the edge detection algorithm and the Prewitt operator algorithm. The average segmentation time results are shown in Table 1. The average

segmentation time of the proposed algorithm is 2.56s, which is 0.16s and 0.3s higher than that of the edge detection algorithm and the Prewitt operator, respectively.

5.3. Comparison of ratio IoU of the Algorithm

As shown in Table 2, the average segmentation and intersection ratio of IoU of image one is 0.98, which is 17% and 23% higher than the other algorithms. The IoU ratio of this algorithm for image two is 0.97, which is 0.34 and 0.19 higher than the other algorithms for image two.

Table 2: Comparison table of algorithm ratio of IoU

Image	Edge Detection	Prewitt Operator	Our improved algorithm
Lung image one	0.81	0.75	0.98
Lung image two	0.78	0.63	0.97

5.4. Segmentation performance of the algorithm with different iterations

In order to evaluate the efficiency of the structure of algorithm and compare the effect of different iterations on the segmentation performance. The specific segmentation performance index is shown in Figure7 in the comparison experiment.

In order to confirm the efficiency of different iterations for lung image segmentation in this paper, we take four evaluation metrics, PA, MPA, MIoU, and IoU. The 400 iterations is compared with other number iterations on the Kaggle dataset. The comparison results are reflected in Figure7. The PA, MPA, MIoU, and IoU values of the 400 iterations are reached to 98.54%, 97.24%, 96.11%, and 98.1%. Compared with other number iterations, the performance of 400 iterations achieve more accurate results on PA, MPA, MIoU, and IoU.

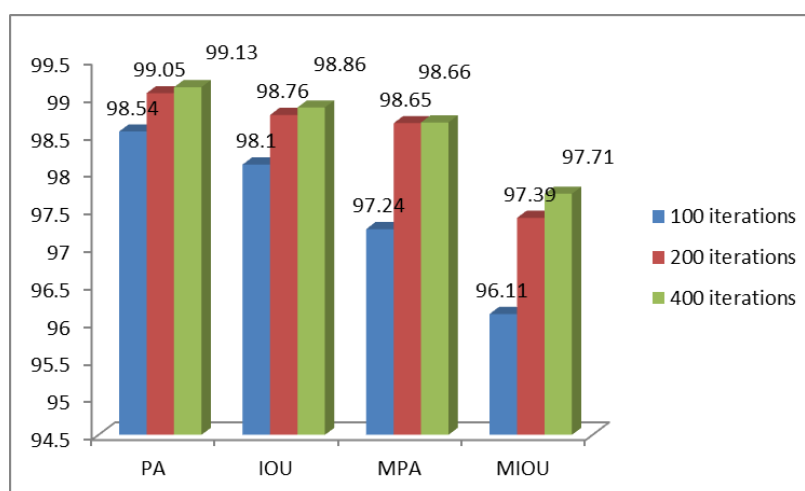


Figure 7: Segmentation performance of different iterations

6. Conclusions

In this paper, the marker-based watershed method and the level set method are improved based on current research progress and reasonable experimental comparisons through an introductory theoretical study and comparison of multi-scale morphological gradient operators. Some aspects of the main work of this paper are presented below: (1) The watershed algorithm is studied and the algorithm is improved by pre-processing the watershed algorithm based on control markers to solve the problem of image over-segmentation as far as practicable. (2) The improved watershed labelling algorithm and the improved watershed algorithm are combined, and a method for segmenting images using the watershed algorithm and the level set algorithm is proposed. To achieve this, the preliminary evolution curve of the level set algorithm is extracted as the segmentation result of the watershed algorithm with the largest connected region.

Acknowledgements

I would like to thank Ningbo University of Finance and Economics for helpful discussions on topics related to this work.

References

- [1] Pham DL, Xu C, Prince JL.: A survey of current methods in medical image segmentation. *Annu Rev Biomed Eng*, 2000, 2, pp.315–338
- [2] Wu HB. :Research on image segmentation algorithm based on watershed and level set method. Hunan Province, Central South University, 2009, 11, (12), pp.202-234
- [3] Maragos P.:Differential morphology and image processing. *IEEE Trans Image Processing.*, 1996, 5, (6), pp. 922-937
- [4] Yang, yong., Ma, zhiming., Xu, chun.:Application of LCV model in medical image segmentation, *Journal of Graphics and Image.*, 2010, 36, (10), pp. 184-186
- [5] Li CM, Xu CY, Gui CF et al.Level Set Evolution Without Reinitialization: A New Variational Formulation. *Computer Vision & Pattern.recognition.*2005, 1, pp.430-436
- [6] Ma, YL., Ma, HY., Chu, PC. : Demonstration of Quantum Image Edge Extraction Enhancement Through Improved Sobel Operator, *IEEE ACCESS.*, 2020, 10, (8), pp. 210277-210285
- [7] Ye, XH., Wang, QY.:Active Contour Image Segmentation Method for Training Talents of Computer Graphics and Image Processing Technology. *IEEE ACCESS.*, 2021, 121, (9), pp. 19187-19194
- [8] Nagornov, NN., Lyakhov, PA., Valueva, MV., Bergerman, MV.: RNS-Based FPGA Accelerators for High-Quality 3D Medical Image Wavelet Processing Using Scaled Filter Coefficients, *IEEE ACCESS.*, 2022, 57, (10), pp. 19215-19231
- [9] Bengtsson, E., Lindblad, J.: Robust cell image segmentation methods, *Pattern Recognition and Image Analysis.*, 2004, 12, (2), pp.157-167
- [10] Guanmin, L. :A Multiscale Algorithm for Computing Image Morphological Gradient, *Chinese Journal of Image and Graph-ic.*, 2001, 6, (3), pp. 214-218.
- [11] Xin, L.:A Degree-Controlled Morphological Multiscale Gradient Watershed Algorithm, *Application Research of Comput-ers*, 2008, 25, (2), pp. 475-478.
- [12] Lankton, S., Tannenbaum, A.: Localizing Region-based Active Contours, *IEEE Transactions on Image Processing*, 2008, 17, (11), pp.2029-2039.
- [13] Canny, J.: A Computational Approach to Edge Detection, *IEEE Trans on Pattern Analysis and Machine Intelligence.*, 1986, 8, (6), pp. 679-698
- [14] Kim, J ., Kang, S. :Model-Agnostic Post-Processing Based on Recursive Feedback for Medical Image Segmentation, *IEEE AC-CESS*, 2021, 5, (9), pp. 157035-157042
- [15] Kowal, M., Zejmo, M., Skobel, M., Korbicz, J., Monczak, R.:Cell Nuclei Segmentation in Cytological Images Using Convo-lu-tional Neural Network and Seeded Watershed Algorithm, *Journal Of Digital Imaging.*, 2020, 33, (1), pp. 231-242
- [16] Zhang, HT., Li, YN.: Watershed algorithm with threshold mark for color image segmentation, *Journal of Image and Graphics.*, 2015, 20, (12), pp.1602-1611
- [17] Heshmati, A., Gholami, M., Rashno, A.:Scheme for unsupervised colour-texture image segmentation using neutrosophic set and non-subsampled contourlet transform, *IET Image Processing.*, 2016, 10, (6), pp.464-473
- [18] Jie, L., Min, D., Pengfeng, X.: Multi-scale watershed segmentation of high-resolution multispectral remote sensing images using wavelet transform, *Acta Remote Sensing.*, 2011, 15, (5), pp. 908-926.
- [19] Flores, FC., Lotufo, RA.: Watershed from propagated markers: an interactive method to morphological object segmentation in image sequences, *Image and Vision Computing .*, 2010, 28, (11), pp. 1491-1514.
- [20] Wang, JQ., Yao, PP., Liu, WL., Wang, XL.: A Hybrid Method for the Segmentation of a Ferrograph Image Using Mark-er-Controlled Watershed and Grey Clustering, *Tribology Transactions.*, 2016, 59, (3), pp. 513-521
- [21] Li, DR., Li, Deren., Zhang, GF., Wu, ZC., Yi, LN.: An Edge Embedded Marker-Based Watershed Algorithm for High Spatial Resolution RemoteSensing Image Segmentation, *IEEE Transactions On Image Processing.*, 2010, 19, (10), pp. 2781-2787
- [22] Yanwei, C., Hongxia, C.: Image Segmentation Algorithm based on two-dimensional OSTU of Color Space, *Electronic Design Engineering.*, 2014, (05), pp. 131–133
- [23] Wang, DM: A multiscale gradient algorithm for image segmentation using watersheds, *Pattern Recognition*, 1997, 30 ,(12) , pp.2043-2052

- [24] Cao, MY., Wang, S., Wei, L. et al.: *Segmentation of immunohistochemical image of lung neuroendocrine tumor based on double layer watershed*, *Multimedia Tools And Applications.*, 2019, 78, (7), pp. 9193-9215
- [25] Guo, YH., Sengur, A., Akbulut, Y., Shipley, A.: *An effective color image segmentation approach using neutrosophic adaptive mean shift clustering*, *Measurement.*, 2018, (119), pp. 28-40
- [26] Otsu, N.: *A threshold selection method from gray-level histogram*, *IEEE Trans on Systems Man and Cybernet.*, 1979, 9, (1), pp. 62-66
- [27] Weilin, W., Jinyong, L., Shu, W. et al.: *A Novel Multiphoton Microscopy images segmentation method based on superpixel and watershed*, *Journal of Biophotonics.*, 2017, 10, (4), pp. 532-541
- [28] Zhang, JX., Zhang, KP., Wu, JK., Hu, XD.: *Color segmentation and extraction of yarn-dyed fabric based on a hyperspectral imaging system*, *Textile Research Journal.*, 2021, 91, (7), pp. 729-742
- [29] Liu, TG., Miao, QG., Tian, K. et al.: *SCTMS: Superpixel based color topographic map segmentation method*, *Journal of Visual Communication and Image Representation.*, 2016, (35), pp. 78-90
- [30] Li, G., Shuyuan, Y., Haiqiang, L.: *New Unsupervised Image Segmentation via Marker-Based Watershed*, *Journal of Image and Graphics.*, 2007, 12, (6), pp. 1025-1032